New directions in gauge topology from lattice simulations

Speaker: **Claudio Bonanno**
Galileo Galilei Institute for Theoretical Physics
✉ claudio.bonanno@pi.infn.it

Based on: CB, Clemente, D'Elia, Sanfilippo, 2019 [arXiv:1908.11832];
Berni, CB, D'Elia, 2019 [arXiv:1911.03384];
Berni, CB, D'Elia, 2020 [arXiv:2009.14056]; CB, Bonati, D'Elia, 2020 [arXiv:2012.14000];
Athenodorou, CB, Bonati, et al., 2021 [arXiv:2112.02982]

GGI Post-Doc Day 2021 - Dec. 17th 2021

The topological charge in $4d$ gauge theories

The topological charge of the gluon field $A_\mu(x)$

$$Q = \frac{g^2}{16\pi^2}\int d^4x \ \mathrm{Tr}\left\{\widetilde{G}^{\mu\nu}(x)G_{\mu\nu}(x)\right\} \in \mathbb{Z}, \qquad \widetilde{G}^{\mu\nu}(x) \equiv \frac{1}{2}\varepsilon^{\mu\nu\rho\sigma}G_{\rho\sigma}(x)$$

can be coupled to the QCD action via the dimensionless parameter θ:

$$S_{QCD} \to S_{QCD}(\theta) = S_{QCD} + \theta Q,$$

introducing a **non-trivial dependence on θ** in the theory.

The θ-dependence of the free energy (density), defined in Euclidean time as

$$f(\theta) = -\frac{1}{V}\log\int [d\overline{\psi}d\psi dA]e^{-S_{QCD}+i\theta Q}, \qquad f(\theta) = \frac{1}{2}\chi\theta^2\left(1+\sum_{n=1}^{\infty} b_{2n}\theta^{2n}\right),$$

$$\chi = \left.\frac{\langle Q^2\rangle}{V}\right|_{\theta=0}, \qquad b_2 = -\frac{1}{12}\left.\frac{\langle Q^4\rangle - 3\langle Q^2\rangle^2}{\langle Q^2\rangle}\right|_{\theta=0}, \qquad b_{2n} \propto \left.\frac{\langle Q^{2n+2}\rangle_c}{\langle Q^2\rangle}\right|_{\theta=0}$$

has been extensively investigated in several different physical contexts.

Physical relevance of θ-dep. in QCD and related theories

- CP-**symmetry breaking and Beyond Standard Model physics**: non-zero $\theta \to$ breaking of CP symmetry, e.g., non-zero neutron Electric Dipole Moment (nEDM).
    - Experiments: nEDM is well compatible with zero $\implies$ $\theta \sim 0$ within 10^{-10} $\implies$ No strong-CP violation.
    - If CP symmetry is conserved $\implies$ fine-tuning problem on θ: **strong-**CP **problem**. Simple and promising solution: axion. Axion physics related to θ-dependence in QCD.
- **Large-N limit and hadron physics**: Q **breaks** the $U(1)_A$ flavor symmetry through **anomaly** $\implies$ large mass of η' meson. Physical parameters of the η' related to θ-dependence of large-N $SU(N)$ gauge theories.
- **Large-N and θ-dep. of lower dim. gauge theories**: e.g., $2d$ CP^{N-1} models. Extensively studied both **analytically** ($1/N$ expansion) and on the **lattice** (cheap to simulate) as test-beds for validation of *Lattice QCD* numerical methods.

The lattice approach is effective in addressing these physical aspects. However, there are several non-trivial computational problems to be faced.

Topological Freezing

Approaching the continuum limit, fluctuations of Q during the simulation become extremely rare. In the continuum theory topological sectors are separated by infinite free-energy barriers.

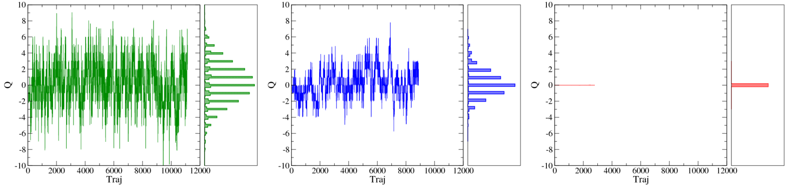

Left to right: $a = 0.082$ fm, 0.057 fm and 0.040 fm (figs. Bonati et al., 2016)

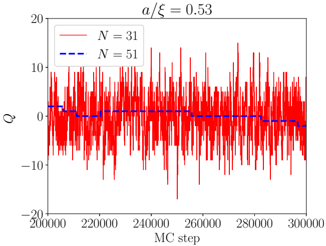

Moreover, topological freezing worsens increasing N (example for CP^{N-1} models, also occurs in $SU(N)$ gauge theories) $\Longrightarrow$ approaching the continuum limit for N large is extremely challenging.

Chiral symmetry and large lattice artifacts for χ

Gauge field configurations are weighted with the determinant of $\not{D}$ in the path integral:

$$Z_{QCD} = \int [dA] e^{-S_{YM}} \prod_f \det\{\not{D} + m_f\}, \qquad \det\{\not{D} + m_f\} = \prod_\lambda (i\lambda + m_f)\,.$$

The Index Theorem relates the number of zero-modes n_0 of $\not{D}$ to the topological charge Q of the gauge field $\implies$ suppression of $Q \neq 0$ contributions as the quark mass

$$Q[A] = n_0^{(left)} - n_0^{(right)} \implies \det\{\not{D}[A] + m_f\} \propto m_f^{n_0}$$

On the lattice, $\not{D}_L$ has no exact zero-modes: $\lambda_{would-be-zero} = m_f + i\lambda_0$ $\implies$ suppression of $Q \neq 0$ contributions not effective as in the continuum $\implies$ large corrections to the continuum limit, especially at high T, where we expect $\chi \sim T^{-\alpha}$

(fig. from Bonati et al., 2018, $T \simeq 2.8 T_c$)

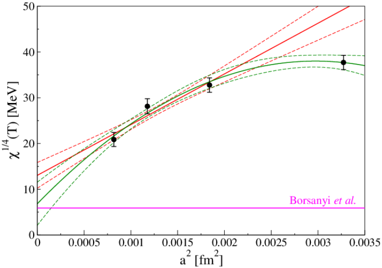

Spectral projectors for χ at high-T (QCD prelim. results)

In the continuum, Q is related to zero-modes of $\not{D}$. Define Q_L by summing eigenmodes of $\not{D}_L$ up to a given threshold M:

$$Q = \mathrm{Tr}\{\gamma_5\} \longrightarrow \mathrm{Tr}\{\gamma_5 \mathbb{P}_M\},$$

$$\mathbb{P}_M = \textstyle\sum_{|\lambda_k| \le M} u_k u_k^\dagger, \qquad \not{D}_L u_k = i\lambda_k u_k.$$

Tuning the value of M allows to reduce lattice corrections because only modes with magnitude $|\lambda| \le M$ are included in the determination of χ.

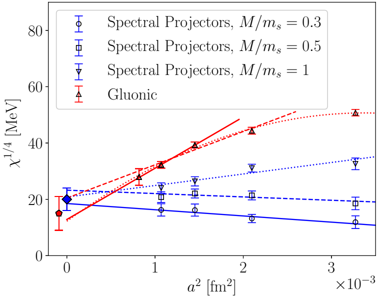

- Threshold mass M simply fixed in terms of one of the quark masses.
- Spectral projectors are affected by much smaller corrections to the continuum limit compared to the standard gluonic definition.
- Magnitude and sign of corrections tunable choosing M/m_s.
- Stable continuum limit varying M/m_s.

Simulate collection of lattice copies with different **boundary conditions**, interpolating periodic and open ones. Each replica has an independent evolution and different copies are swapped from time to time. Charge is quickly changed in the open replica, then the configuration is transferred to the periodic replica through the swaps (Hasenbusch, 2018).

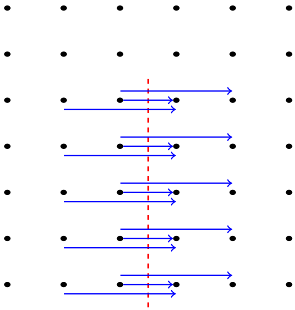

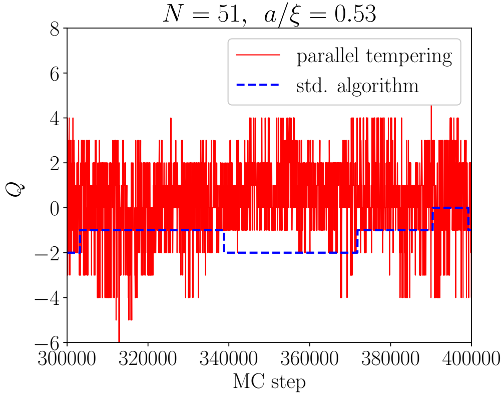

Large-N behavior of $N\xi^2\chi$ in $2d$ CP^{N-1} models

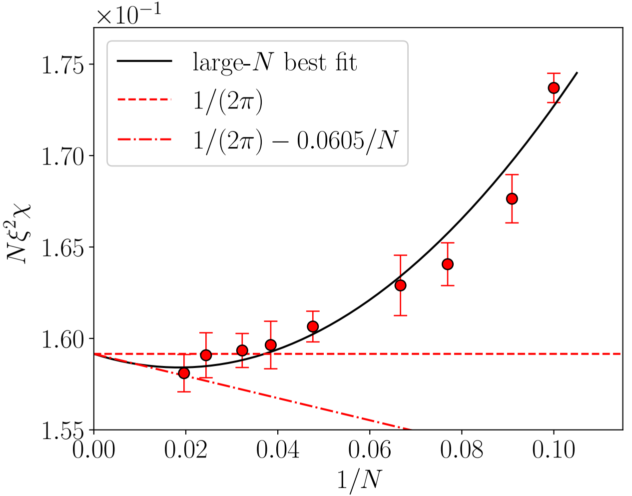

Fit results up to $O(1/N^2)$ terms, $N \in [10, 51]$

$$N\xi^2\chi = 1/(2\pi) - 0.08(2)(1/N) + 2.2(3)(1/N^2)$$

Large-N behavior of $N^2 b_2$ in $2d$ CP^{N-1} models

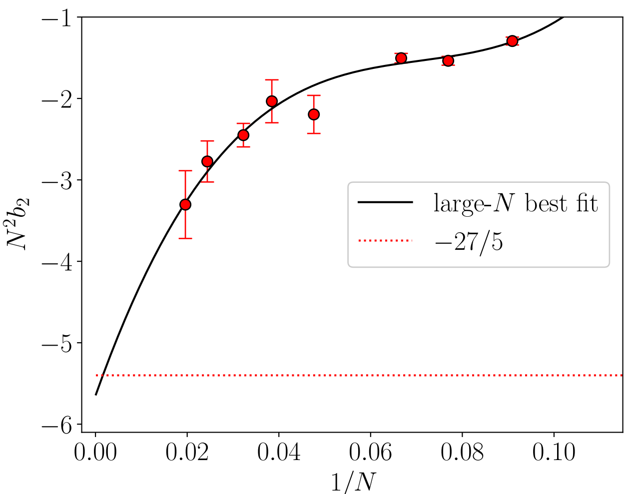

Fit results up to $O(1/N^3)$ terms, $N \in [11, 51]$

$$\bar{b}_2^{theo} \equiv \lim_{N \to \infty} N^2 b_2 = -27/5 = -5.4,$$

$$(N^2 b_2)_{fit} = -5.7(1.1) + 160(60)(1/N) + \ldots$$

Adapting Hasenbusch Algorithm to $4d$ gauge theories

Standard simulations of $SU(N)$ gauge theories suffer from severe CSD in the large-N limit $\implies$ Hasenbusch algorithm can be adopted to mitigate topological freezing. Difference: now the defect is a **cubic volume**.

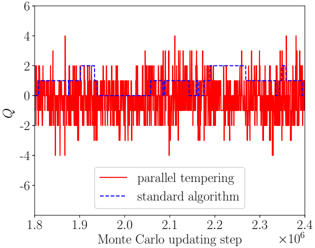

Parallel tempering dramatically improves simulations at large N (fig. on the left: $N = 6$). Performances are exceedingly better without much tuning of the algorithm free parameters (defect volume and swap acceptance).

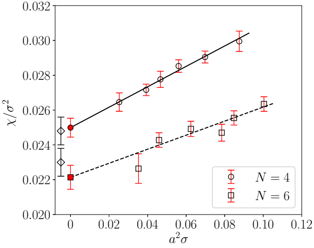

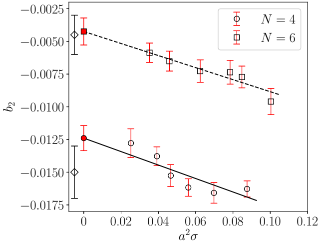

Continuum limits: diamond pnts (Bonati et al., 2016), full pnts (CB, Bonati, D'Elia, 2020).

Large-N limit of χ in $SU(N)$ pure-gauge theories

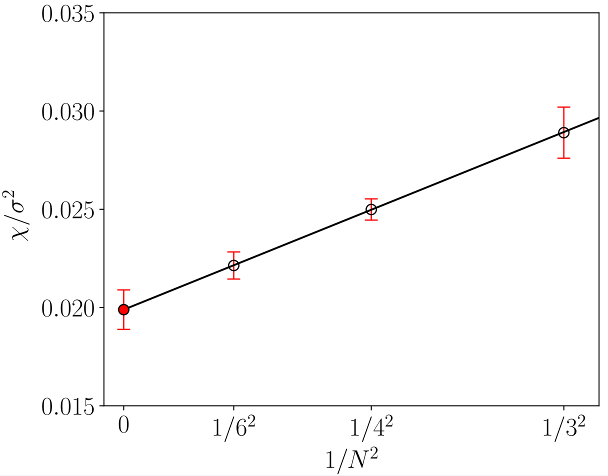

Witten–Veneziano: $\bar{\chi}^{1/4} \simeq 180\ \mathrm{MeV} + O(1/N^2)$. Fit results:

$$\chi/\sigma^2 = 0.0199(10) + 0.08(2)(1/N^2)$$

$$\bar{\chi}/\sigma^2 = 0.0199(10) \implies \bar{\chi}^{1/4} = 173(8)\ \mathrm{MeV}$$

Large-N limit of b_2 in $SU(N)$ pure-gauge theories

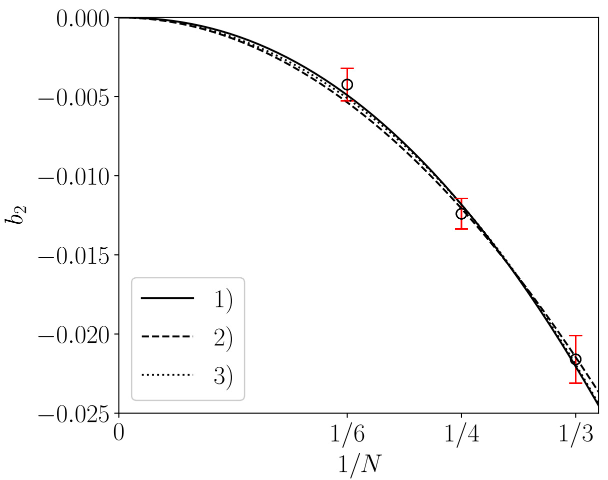

Large-N prediction: $b_2 = \bar{b}_2/N^2 + O(1/N^4)$. Fit results:

1) $b_2 = \bar{b}_2/N^{\gamma} \rightarrow \gamma = 2.17(26)$, cf. $\gamma = 2.0(4)$ (Bonati et al., 2016)
2) $b_2 = \bar{b}_2/N^2 \rightarrow \bar{b}_2 = -0.19(1)$, cf. $\bar{b}_2 = -0.23(3)$ (Bonati et al., 2016)
3) $b_2 = \bar{b}_2/N^2 + \bar{b}_2^{(1)}/N^4 \rightarrow \bar{b}_2^{(1)} = -0.17(35)$

Other topological observables: the susceptibility slope χ'

The 2-point correlator $\widetilde{G}(p^2)$ of topological charge density $q(x)$ is another interesting topological observable (e.g., related to sphaleron rate):

$$\widetilde{G}(p^2) = \int d^4x\, e^{ip\cdot x} \langle q(x)q(0)\rangle\,, \qquad Q = \int d^4x\, q(x)$$

$$\widetilde{G}(p^2=0) = \int d^4x\, \langle q(x)q(0)\rangle = \frac{\langle Q^2\rangle}{V} = \chi$$

$$\frac{d\widetilde{G}}{dp^2}(p^2=0) = -\frac{1}{8}\int d^4x\, |x|^2 \langle q(x)q(0)\rangle \equiv -\frac{1}{8}\chi'$$

No results from the lattice for χ'. Known in some approximations: large-N $2d$ CP^{N-1} up to $O(1/N^2)$, $T=0$ $N_f=3$ QCD through LO Chiral Pert. Theory.

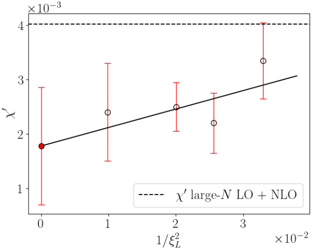

Preliminary results for $2d$ CP^{10} from the lattice: **good agreement** with large-N prediction if NLO corrections are included $\Longrightarrow$ χ' seems to approach large-N limit slowly.
Results will be refined and completed in a forthcoming work.

Conclusions and take-home results

Topology in high-T QCD from spectral projectors

- Spectral Projectors provide an improved technique to compute the continuum limit of χ in high-T QCD.
- Lattice corrections to the continuum limit showed by Spectral Projectors are reduced compared to the standard gluonic definition.
- Lattice corrections of Spectral Projectors can be tuned with a suitable choice of M.

Large-N limit and $1/N$ expansion: $2d$ CP^{N-1} vs $4d$ $SU(N)$ YM

- The Hasenbusch algorithm dramatically mitigates severe Topological Freezing, both in $2d$ CP^{N-1} models and in $4d$ $SU(N)$ gauge theories.
- Large-N data show slow convergence of $1/N$ series of CP^{N-1} models, explaining discrepancies between early lattice results and analytic predictions.
- Large-N predicted scaling of $4d$ $SU(N)$ θ-dependence holds for $N \geq 3$.

Future outlooks

- Refinement of present study of χ' in large-N CP^{N-1} models and future extension to $SU(N)$ gauge theories and full QCD.
- Computation of non-topological observables of large-N $SU(N)$ gauge theories may be affected by topological freezing (e.g., glueball masses) $\implies$ possible improvements of state of the art adopting the Hasenbusch algorithm.
- Adapt Hasenbusch algorithm to full QCD to improve high temperature simulations, which suffer for severe topological freezing when $T \gg T_c$.

Thank you for your attention!

Back-up slides

Signal-to-Noise Ratio (SNR) of b_{2n} (higher-order cumulants) degrades rapidly as the volume grows due to the Central Limit Theorem.

$\implies$ large statistics required to keep finite-size effects of b_{2n} under control.

Idea 1: add imaginary-θ term to Euclidean action, so that it acts as a source term for Q, enhancing SNR of higher-order cumulants:

$$S \to S + \theta_I Q, \quad \theta_I \equiv i\theta \qquad \implies \qquad k_n \to k_n(\theta_I) \propto \frac{d^n f(\theta_I)}{d\theta_I^n}$$

Idea 2: information on χ and b_{2n} now encoded in θ_I-dependence of lower-order cumulants $\implies$ extract χ and b_{2n} from combined fit of θ_I-dependence of cumulants k_n. (N. B. odd cumulants non-zero for $\theta_I \neq 0$)

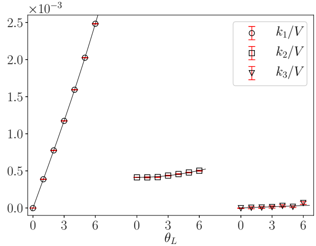

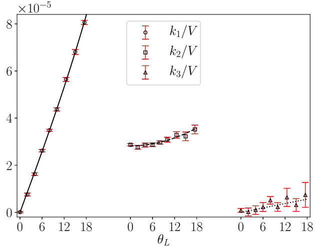

Imaginary-θ fit. Left: $2d$ CP^{N-1} models. Right: $4d$ $SU(N)$ pure-gauge theories.

Hasenbusch algorithm details, $SU(N)$ gauge theories

Links crossing the defect get their coupling multiplied by a factor $c(r)$: $0 \leq c(r) \leq 1$ (r = replica index). In our $SU(N)$ implementation we chose $c(r)$ so that swap acceptance p is $\sim$ const. for couples $(r, r+1)$.

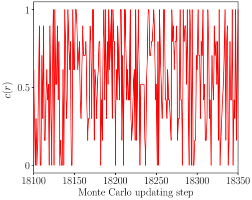

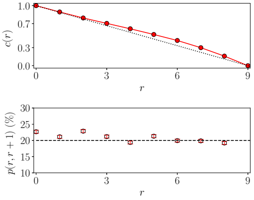

When acc. $\sim$ const. $\Longrightarrow$ conf. moves freely among different replicas (left fig.) and $c(r)$ deviates from linear interpolation (center fig.). Examples: $N = 4$.

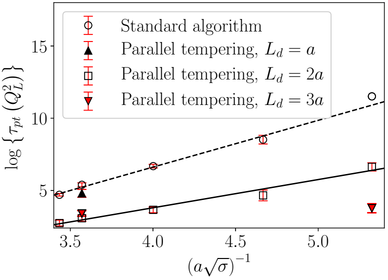

Auto-correlation time of Q^2 scales as $\exp(1/a)$ if defect size L_d is fixed in lattice units as $a \to 0$, however with a **much smaller** slope compared to the standard algorithm. If instead L_d is kept fixed in physical units, scaling with a is **largely improved**. (Fig. on the left: $N = 6$)

Large-N behavior of b_4 in $2d$ CP^{N-1} models

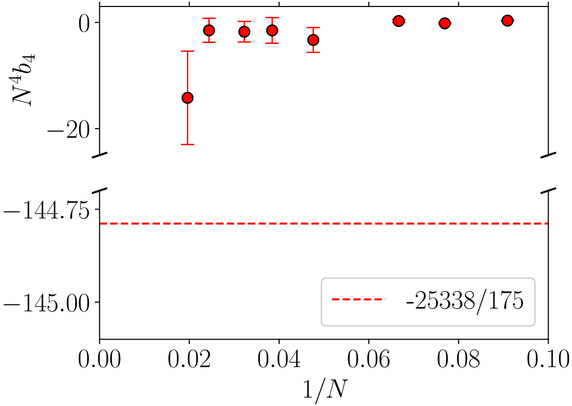

With our statistics $b_4 \sim \langle Q^6 \rangle$ is always compatible with zero. However, we find $|\bar{b}_4| \sim |N^4 b_4| \lesssim 20$, but large-$N$ analytic computations yield $\bar{b}_4 = -25338/175 \simeq -144.79\ldots \implies b_4$ data compatible with slow convergence of $1/N$ series too.